BIOCHEMISTRY
including biophysical chemistry & molecular biology

Article

pubs.acs.org/biochemistry

Short Hydrogen Bond between Redox-Active Tyrosine Y_Z and D1-His190 in the Photosystem II Crystal Structure

Keisuke Saito,[†] Jian-Ren Shen,[‡] Toyokazu Ishida,[§] and Hiroshi Ishikita*[,†,∥]

[†]202 Building E, Career-Path Promotion Unit for Young Life Scientists, Graduate School of Medicine, Kyoto University, Yoshida-Konoe-cho, Sakyo-ku, Kyoto 606-8501, Japan

[‡]Division of Bioscience, Graduate School of Natural Science and Technology/Faculty of Science, Okayama University, Okayama 700-8530, Japan

[§]Nanosystem Research Institute (NRI), National Institute of Advanced Industrial Science and Technology (AIST), Tsukuba Central 2, 1-1-1 Umezono, Tsukuba, Ibaraki 305-8568, Japan

[∥]Japan Science and Technology Agency (JST), PRESTO, 4-1-8 Honcho Kawaguchi, Saitama 332-0012, Japan

Supporting Information

ABSTRACT: The crystal structure of photosystem II (PSII) analyzed at a resolution of 1.9 Å revealed a remarkably short H-bond between redox-active tyrosine Y_Z and D1-His190 (2.46 Å donor−acceptor distance). Using large-scale quantum mechanical/molecular mechanical (QM/MM) calculations with the explicit PSII protein environment, we were able to reproduce this remarkably short H-bond in the original geometry of the crystal structure in the neutral [$Y_ZO\cdots\mathbf{H}\cdots N_\varepsilon$-His-$N_\delta\mathbf{H}\cdots O$═Asn] state, but not in the oxidized states, indicating that the neutral state was the one observed in the crystal structure. In addition to the appropriate redox/protonation state of Y_Z and D1-His190, we found that the presence of a cluster of water molecules played a key role in shortening the distance between Y_Z and D1-His190. The orientations of the water molecules in the cluster were energetically stabilized by the highly polarized PSII protein environment, where the Ca ion of the oxygen-evolving complex (OEC) and the OEC ligand D1-Glu189 were also involved.

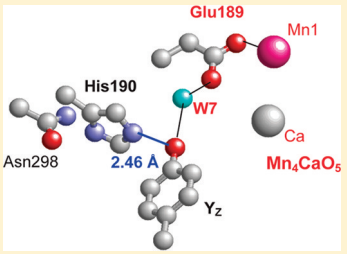

The reaction center of Photosystem II (PSII) consists of the D1/D2 heterodimer, harboring the P_{D1}/P_{D2} chlorophyll *a* (Chl*a*) pair, the Chl_{D1}/Chl_{D2} accessory Chl*a* pair, two pheophytin *a* species ($Pheo_{D1}$ and $Pheo_{D2}$), two quinones, and two additional Chl*a* species [$Chl_{Z(D1)}$ and $Chl_{Z(D2)}$] as the redox-active cofactors. P680, which absorbs light at a wavelength of 680 nm, is formed among the four central Chl*a* molecules, P_{D1}, P_{D2}, Chl_{D1}, and Chl_{D2}. Excitation of P680 leads to the formation of the $Chl_{D1}^{\bullet+}Pheo_{D1}^{\bullet-}$ state,[1,2] followed by the $[P_{D1}/P_{D2}]^{\bullet+}Pheo_{D1}^{\bullet-}$ state. The resulting $[P_{D1}/P_{D2}]^{\bullet+}$ state serves as an electron abstractor for the oxygen-evolving cluster (OEC) via the redox-active tyrosine D1-Tyr161 (Y_Z). The released proton remains near Y_Z, i.e., between Y_Z and D1-His190 (reviewed in ref 3). Upon oxidation by P680, Y_Z transforms from the protonated Y_ZOH state[4,5] to the deprotonated neutral radical state $Y_ZO^\bullet$ in the presence of the neutral state of D1-His190 above pH ∼7. Below pH ∼7, oxidation of Y_Z may result in a positively charged (protonated) state in OEC-depleted PSII as suggested by spectroscopic studies[6] (Figure 1), although the extent to which this is relevant to native PSII is not clear at present.[7−9] Because of the significant involvement of Y_Z in the four-electron and four-proton abstraction reactions from $2H_2O$ to yield O_2, its redox and protonation properties have attracted considerable attention.[10,11]

Recently, the PSII crystal structure from *Thermosynechococcus vulcanus* was reported at a resolution of 1.9 Å, which revealed all of the components of the OEC cluster, giving rise to a chemical formula of Mn_4CaO_5.[12] In addition, all of the amino acid ligands of the OEC cluster were unambiguously assigned, and a number of bound water molecules, in particular those in the neighborhood of the OEC cluster and Y_Z, were reported for the first time. The 1.9 Å structure confirmed that the OH group of Y_Z was an H-bond distance from N_ε of D1-His190. Most strikingly, the donor−acceptor distance of this H-bond (O_{Y_Z}−$N_{\varepsilon,His}$ distance) is very short, 2.46 Å based on Protein Data Bank (PDB) entry 3ARC (Figure 2) (a value of 2.5 Å was reported in ref 12 because of the estimated experimental uncertainty of 0.16 Å). The assignment of the atoms of Y_Z and D1-His190 appears to be quite reliable because the *B* factors of Y_Z (22.4 for hydroxyl O), D1-His190 (22.4 for N_ε and 23.3 for N_δ), and water molecules in the neighborhood (25.5 for W7[13]) were relatively small for membrane proteins. In comparison with the corresponding distances of 2.78 Å in the previous 3.0 Å structure,[14] 2.67 Å in the previous 2.9 Å structure,[15] and 2.82,[16] 2.83,[17] and 2.88 Å[18] in the geometry-optimized Tyr-His model complexes, the O_{Y_Z}−$N_{\varepsilon,His}$ distance of 2.46 Å in the 1.9 Å structure is unusually short. It is therefore interesting to see

Received: August 30, 2011
Revised: October 5, 2011
Published: October 5, 2011

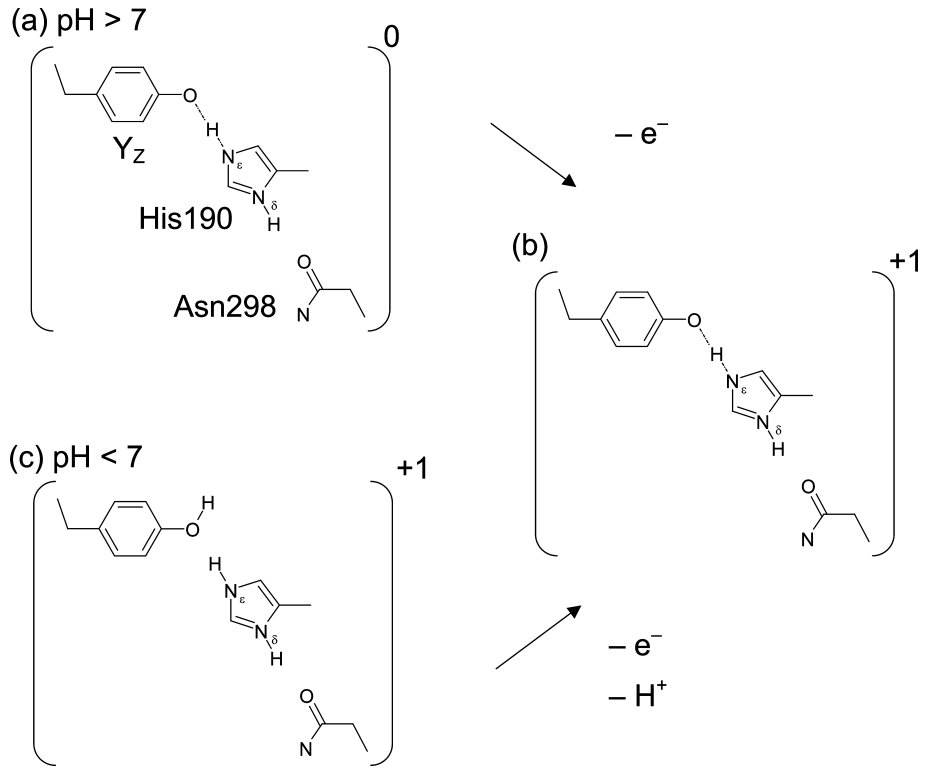

Figure 1. Reaction scheme of photooxidation of Y_Z.[6]

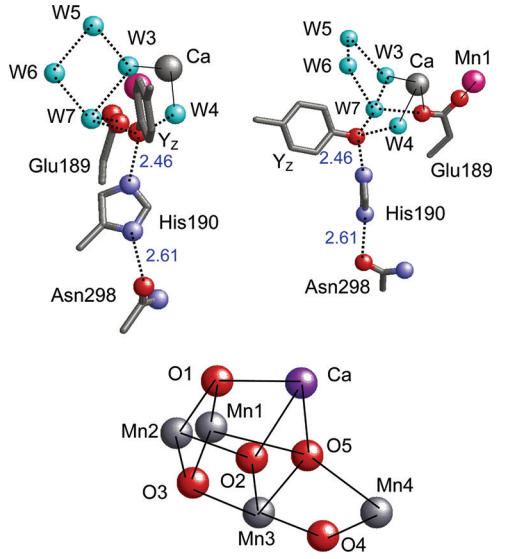

Figure 2. Geometry of Y_Z, D1-His190, D1-Asn298, and a cluster of water molecules identified in the 1.9 Å structure (top), viewed from two different orientations. H-Bonds and ligations are represented as dotted and solid lines, respectively. For numbering of water molecules, see ref 13. Atomic composition of the OEC cluster (bottom).

how this short H-bond is energetically possible and what makes this distance so short.

In this study, we used a large-scale quantum mechanical/molecular mechanical (QM/MM) approach to investigate the dependencies of the H-bond distance between Y_Z and D1-His190 on the protonation states of the two residues and found that the short distance observed in the crystal structure was reproduced in only one specific protonation state. Consideration of a cluster of water molecules near Y_Z and the OEC cluster in the QM region allowed us to identify the factors that contributed to the short H-bond, which are also important for maintaining the intactness of the OEC structure.

COMPUTATIONAL PROCEDURES

As demonstrated in the previous article,[19] we employed the following systematic modeling procedure. First, we constructed a realistic molecular model of the whole PSII complex using the recent high-resolution crystal structure. Second, to gain a better understanding of the electronic structure of Y_Z, D1-His190, D1-Asn298, and the water molecules in the neighborhood, we performed large-scale QM/MM calculations for the PSII protein. Technical details of each modeling procedure are summarized below.

Coordinates. The atomic coordinates of PSII were taken from the X-ray structure of the PSII complexes from *T. vulcanus* at 1.9 Å resolution (PDB entry 3ARC).[12] Hydrogen atoms were generated and energetically optimized with CHARMM.[20] On the other hand, the positions of all non-hydrogen atoms were fixed and all titratable groups were kept in their standard protonation states; i.e., acidic groups were ionized, and basic groups were protonated. For the QM/MM calculations, we added additional counterions to neutralize the whole system.

Atomic Partial Charges. Atomic partial charges of the amino acids were adopted from the all-atom CHARMM22[21] parameter set. The atomic charges of Chl*a*, Pheo*a*, and quinones were determined by fitting the electrostatic potential in the neighborhood of these molecules using the RESP procedure.[22] The electronic wave functions were calculated after the optimization of the geometry with the DFT module in JAGUAR[23] (B3LYP/LACVP*). The OEC models employed, including the atomic charges and the protonation states, are described below.

dx.doi.org/10.1021/bi201366j | *Biochemistry* 2011, 50, 9836–9844

Table 1. H-Bond Distances (in angstroms) for Y_Z in QM/MM Optimized Geometries (B3LYP/LACVP**+) in the PSII Protein Environment in the $(O4)^{2-}(O5)H^-$ Model[a]

redox state	O_Y–$N_{\varepsilon,His}$	O_Y–H	H–$N_{\varepsilon,His}$	O_Y–O_{W7}	$N_{\delta,His}$–O_{Asn}	rmsd
original (1.9 Å structure)	2.46	–[b]	–[b]	2.62	2.60	
$[Y_ZO\cdots\mathbf{H}\cdots N_\varepsilon\text{-His-}N_\delta\mathbf{H}\cdots O{=}Asn^c]^0$	2.47	1.13	1.34	2.61	2.64	0.134
	2.47	1.31	1.17	2.58	2.63	0.130
$[Y_ZO\cdots\mathbf{H}\cdots N_\varepsilon\text{-His-}N_\delta\mathbf{H}\cdots O{=}Asn^c]^+$	2.70	1.69	1.03	2.69	2.57	0.150
$[Y_ZOH^d\cdots\mathbf{H}N_\varepsilon\text{-His-}N_\delta\mathbf{H}\cdots O{=}Asn^c]^+$	2.70	1.68	1.03	2.80	2.56	0.166

[a]The H-atom positions between the H-bond donor and acceptor atoms are indicated in bold. Abbreviations: O_Y, phenol O atom of Y_Z; $N_{\varepsilon,His}$, N_ε atom of D1-His190 as an H-bond partner of Y_Z; O_{W7}, O atom of crystal water W7; $N_{\delta,His}$, N_δ atom of D1-His190 as an H-bond partner of D1-Asn298; O_{Asn}, side chain O atom of D1-Asn298; rmsd, root-mean-square deviation of the optimized side chain heavy atoms of Y_Z, D1-His190, and D1-Asn298 with respect to those of the 1.9 Å structure. [b]Not applicable. [c]The O atom of the side chain C=O group of D1-Asn298 is the H-bond partner of D1-His190, as seen in the original crystal structure. [d]The H atom of Y_ZOH is not the one in the focusing H-bond (Figure 1c). The O_Y–H distance of Y_ZOH is 1.00 Å.

OEC Models. In the S_1 state, the valences of the four Mn atoms are most probably two at III and two at IV. The formal charges of the OEC components were assumed to be as follows: two Mn ions = +3, another two Mn atoms = +4, Ca = +2, D1-Asp170, Glu189, Glu333, Asp342, Ala344, and CP43-Glu354 = −1 (deprotonated), D1-His332 = 0 (neutral), and CP43-Arg357 = +1 (protonated). The exact valences of the individual Mn atoms are unclear; however, we found that changing the valences of each Mn atom with the same overall charge distribution described above did not affect our calculated results significantly.[19] The protonation states of the O atoms (and thus the net charge of the OEC atoms) in the OEC cluster remain unclear (Figure 2, bottom). Although O1–O3 are likely to be unprotonated O^{2-}, on the basis of the observations of the OEC geometry, the protonation states of O4 linking Mn4 and Mn3 in the Mn_3CaO_4-cubane, and O5 in one of the corners of the cubane linking Mn4 and the cubane, require further investigation as they might be O^{2-}, protonated OH^-, or even H_2O. Although the relevant S state of the OEC cluster in the crystal structure remains open,[24] we considered the OEC cluster as being in the S1 state in this study.

The difference in the net charge or the protonation states of the system did not significantly alter the calculated H-bond donor–acceptor distances among the different models (where the valence of the four Mn atoms remains unchanged), e.g., O_{Y_Z}–$N_{\varepsilon,His}$ distances of 2.47 Å in the $(O4)^{2-}(O5)H^-$ model, 2.46 Å in the $(O4)H^-(O5)H^-$ model, and 2.51 Å in the $(O4)^{2-}H_2(O5)$ model (Table S1 of the Supporting Information). We discuss the $(O4)^{2-}(O5)H^-$ model in this study (for the QM/MM optimized geometries of Y_Z, D1-His190, and D1-Asn298, see Table S2 of the Supporting Information).

QM/MM Calculations. In all QM/MM calculations reported here, we employed the so-called electrostatic embedding QM/MM scheme. In all QM/MM calculations, we used the Qsite[25] program code. Electrostatic as well as steric effects created by the PSII protein environment were explicitly considered in all these calculations. Because of the large size of the system of PSII, we considered residues and cofactors in only subunits D1, D2, CP47, and CP43 and performed the QM/MM calculations in the following two steps.

In the initial QM/MM calculation, the entire OEC cluster was defined as the QM region and the remaining protein subunits and cofactors were defined as the MM region. During the calculation, the heavy atom positions of the QM region were fixed. Because the purpose of the initial QM/MM calculation was to determine the proper H atom positions and/or orientations of the OEC cluster as well as the proper atomic partial charges of the entire OEC cluster, this treatment was accurate enough to describe the electronic structure of the OEC region. In addition, this treatment, without moving the heavy atoms of the OEC cluster, should effectively suppress possible artifacts caused by the uncertainty of the actual redox state (S state) of the OEC cluster in the 1.9 Å structure (e.g., a mixture of states possibly including S_0, S_{-1}, and S_{-2}, as suggested in recent theoretical studies[24]) on the resulting QM/MM optimized atomic coordinates of Mn_4CaO_5. Table S3 of the Supporting Information lists the resulting atomic partial charges of the OEC cluster.

In the final QM/MM calculation, the QM region was redefined as side chains of Y_Z (D1-Tyr161), D1-His190, and D1-Asn298, the Ca of the OEC cluster (note that the Ca position was fixed), and water molecules that are H-bond distances from the side chain N or O atoms of the three key residues (i.e., W3–W7,[13] HOH349, HOH1014, and HOH1117), whereas other protein units and all cofactors were approximated by the MM force field. All of the atomic coordinates in the QM region (including those of the eight water molecules) were fully relaxed (i.e., not fixed) in the final QM/MM calculation. The OEC cluster was included in the MM region with the atom positions and atomic partial charges being fixed to the resulting geometry and/or charges as obtained in the initial QM/MM calculation. We employed the restricted DFT method for describing the closed-shell electronic structure and the unrestricted DFT method for the open-shell electronic structure with the B3LYP functional and LACVP* (for OEC cluster) or LACVP**+ (for Y_Z, D1-His190, and D1-Asn298) basis sets.

For following the proton transfer (PT) pathways, we employed an iterative (constrained) QM/MM geometry optimization that included fixing the selected reaction coordinate. The reaction coordinate was defined as a linear combination of two PT distances (O_{Y_Z}–H and H–$N_{\varepsilon,His}$). Except for the atoms directly involved in the PT reaction coordinate (i.e., O_{Y_Z}, a transferring H, and $N_{\varepsilon,His}$ atoms), all of the atomic coordinates in the QM region (including those of the eight water molecules) were fully relaxed (i.e., not fixed) in the generation of the scans. We did not observe detectable changes in the position of the water molecules during the analysis.

Starting from the QM/MM refined geometry of the initial QM fragment (H is attached to Y_Z), we determined the PT pathway by gradually optimizing the positions of the protons along the selected reaction coordinate with a small step size (0.02 or 0.05 Å). A total of ~20–40 points were determined

along the reaction coordinate by the iterative QM/MM procedure. All stationary structures were confirmed by vibrational frequency calculations, which were performed by a numerical differentiation method at the same level of the QM/MM geometry optimization.

Model Systems for Comparison with the PSII Protein Environment. The atomic coordinates of Tyr-His, Tyr-His-Asn, and Tyr-His-Asp model systems consisted of the amino acid side chains and the methylated C_β atom. The stable geometries were obtained after geometry optimization had been performed with the DFT module in JAGUAR[23] (B3LYP/LACVP**+) in a vacuum. See Table S4 of the Supporting Information for the optimized geometries.

RESULTS AND DISCUSSION

H-Bond/Protonation Pattern Corresponding to the Geometry in the Crystal Structure. Prior to the transfer of an electron from the OEC to P680 via Y_Z, Y_Z is likely to be protonated (Y_ZOH),[4,5] whereas the H-bond partner D1-His190 is likely to be neutral (protonated at the N_δ site) above pH ~7 and positively charged (protonated at both N_ε and N_δ sites) below pH ~7.[6] As a result of the QM/MM geometry optimization, the neutral [$Y_ZO\cdots\mathbf{H}\cdots N_\varepsilon$-His-$N_\delta\mathbf{H}\cdots O{=}$Asn] state [the initial state above pH ~7 (Figure 1a)] resulted in an $O_{Y_Z}-N_{\varepsilon,His}$ distance of 2.47 Å, which reproduced the corresponding distance of 2.46 Å in the 1.9 Å structure (Table 1). We confirmed that the $O_{Y_Z}-N_{\varepsilon,His}$ distance of 2.47 Å exactly corresponded to the energy minimum of the H-bond, by altering the $O_{Y_Z}-N_{\varepsilon,His}$ distance and analyzing the potential energy profile; the energy minimum of the H bond increases either beyond or below the $O_{Y_Z}-N_{\varepsilon,His}$ distance of 2.47 Å (Figure 3a, bottom, and Figure S1 of the Supporting Information).

In contrast, both the positively charged [$Y_ZOH\cdots\mathbf{H}N_\varepsilon$-His-$N_\delta\mathbf{H}\cdots O{=}$Asn $]^+$ state [the initial state below pH ~7 (Figure 1c)] and the positively charged [$Y_ZO\cdots\mathbf{H}\cdots N_\varepsilon$-His-$N_\delta\mathbf{H}\cdots O{=}Asn]^+$ state [the oxidized or product state (Figure 1b)] resulted in a larger distance of 2.70 Å (Table 1). The neutral [$Y_ZO\cdots\mathbf{H}\cdots N_\varepsilon$-His-$N_\delta\mathbf{H}\cdots O{=}$Asn] state also reproduced the H-bond distance between Y_Z and W7 ($O_{Y_Z}-O_{W7}$ distance) better than the other two states. These results indicate that the neutral [$Y_ZO\cdots\mathbf{H}\cdots N_\varepsilon$-His-$N_\delta\mathbf{H}\cdots O{=}$Asn] state is likely to be the relevant state in the 1.9 Å structure. The neutral [$Y_ZO\cdots\mathbf{H}\cdots N_\varepsilon$-His-$N_\delta\mathbf{H}\cdots O{=}$Asn] state possessed different stable states and consisted of [$Y_ZO\mathbf{H}\cdots N_\varepsilon$-His-$N_\delta\mathbf{H}\cdots O{=}$Asn] and [$Y_ZO^-\cdots\mathbf{H}N_\varepsilon$-His-$N_\delta\mathbf{H}^+\cdots O{=}$Asn]. These conformations possess an identical $O_{Y_Z}-N_{\varepsilon,His}$ distance of 2.47 Å. This feature resembles an intermediate state as a mixture of the two Y_ZOH and Y_ZO^- states as suggested by UV−vis spectroscopic studies.[26,27] Because the H atom is always in the vicinity of Y_Z and D1-His190, this model may also account for the protonated Y_ZOH state prior to photooxidation, as suggested by FTIR studies.[4,5]

Panels a and b of Figure 3 show the potential energy profile of PT between Y_Z and D1-His190 in the neutral [$Y_ZO\cdots\mathbf{H}\cdots N_\varepsilon$-His-$N_\delta\mathbf{H}\cdots O{=}$Asn] state and the positively charged [$Y_ZO\cdots\mathbf{H}\cdots N_\varepsilon$-His-$N_\delta\mathbf{H}\cdots O{=}Asn]^+$ state, respectively. As clearly shown in these two profiles, both profiles exhibit different PT characters in qualitative and quantitative fashions; the potential energy curve in the neutral state has a rather symmetric single-well character, whereas an asymmetric

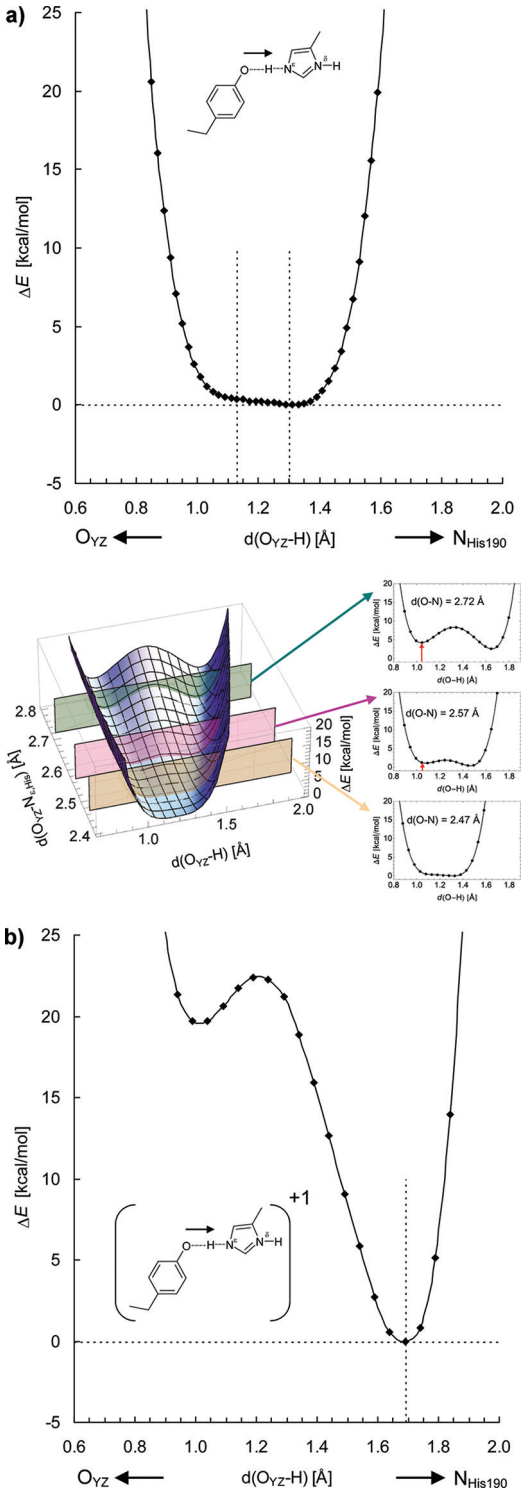

Figure 3. Energy profiles along the PT coordinate for H-bond donor−acceptor pairs in the (a) neutral [$Y_ZO\cdots\mathbf{H}\cdots N_\varepsilon$-His-$N_\delta\mathbf{H}\cdots O{=}$Asn] and (b) positively charged [$Y_ZO\cdots\mathbf{H}\cdots N_\varepsilon$-His-$N_\delta\mathbf{H}\cdots O{=}Asn]^+$ states. ΔE describes the difference in energy relative to the energy minimum. Vertical dotted lines indicate the H atom position listed in Table 2. The red arrow indicates the energy difference from the energy minimum, although it is not always shown. Except for the atoms directly involved in the PT reaction coordinate (i.e., O_{Y_Z}, a transferring H, and $N_{\varepsilon,His}$ atoms), all of the atomic coordinates in the QM region (including those of the eight water molecules) were fully relaxed.

dx.doi.org/10.1021/bi201366j | Biochemistry 2011, 50, 9836−9844

Table 2. Influence of the Deletion of Water Molecules near Y_Z on the H-Bond Distances (in angstroms) in the $(O4)^{2-}(O5)H^-$ Model[a]

	$O_Y-N_{\varepsilon,His}$	O_Y-H	$H-N_{\varepsilon,His}$	O_Y-O_{W7}	$N_{\delta,His}-O_{Asn}$	rmsd
original (1.9 Å structure)	2.46	–[b]	–[b]	2.62	2.60	
Y_ZOH/N_ε-His-$N_\delta H$/O=Asn [c]	2.47	1.13	1.34	2.61	2.64	0.134
W3 deleted	2.49	1.34	1.15	2.62	2.65	0.143
W4 deleted	2.51	1.07	1.44	2.58	2.64	0.141
W5 deleted	2.46	1.14	1.33	2.66	2.64	0.136
W6 deleted	2.46	1.17	1.29	2.59	2.64	0.137
W7 deleted	2.55	1.05	1.51	–[b]	2.66	0.185
W3–W7 deleted	2.67	1.02	1.65	–[b]	2.70	0.229
all waters deleted	2.71	1.01	1.71	–[b]	2.77	0.284

[a]Abbreviations: O_Y, phenol O atom of Y_Z; $N_{\varepsilon,His}$, N_ε atom of D1-His190 as an H-bond partner of Y_Z; O_{W7}, O atom of the crystal water W7; $N_{\delta,His}$, N_δ atom of D1-His190 as an H-bond partner of D1-Asn298; O_{Asn}, side chain O atom of D1-Asn298; rmsd, root-mean-square deviation of the side chain heavy atoms of Y_Z, D1-His190, and D1-Asn298 with respect to the 1.9 Å structure. For atomic coordinates of the QM/MM optimized geometries, see Table S5 of the Supporting Information. [b]Not applicable. [c]The O atom of the side chain C=O group of D1-Asn298 is the H-bond partner of D1-His190, as seen in the original crystal structure.

double-well character for the charged state was observed. The latter is a typical H-bond profile (Figure 3b) in which the proton is localized at the donor side and the typical bond distance is 2.8–3.0 Å. On the other hand, the former represents a typical ionic H-bond character (Figure 3a) in which the proton is delocalized at the bottom of nearly barrierless potential[28] (note that the energy difference between the two states, namely, one with the proton close to the Y_Z moiety and the other with the proton close to D1-His190, is marginal and their energy levels are essentially the same).

Excitation of P680 results in the formation of the $[P_{D1}/P_{D2}]^{\bullet+}$ state that serves as an electron abstractor for the OEC. Because the calculated $P_{D1}^{\bullet+}/P_{D2}^{\bullet+}$ ratio can be significantly influenced by the electrostatic influence of the D1-Asn298/D2-Arg294 residue pair that participates in the H-bond network with Y_Z/Y_D,[19] redox or protonation states of Y_Z/Y_D may also be influenced by the $[P_{D1}/P_{D2}]^{\bullet+}$ state. Thus, we analyzed the potential energy profile of PT between Y_Z and D1-His190 in the $[P_{D1}/P_{D2}]^{\bullet+}$ state, assigning a $P_{D1}^{\bullet+}/P_{D2}^{\bullet+}$ ratio of 76.9/23.1[19] to P_{D1}/P_{D2} of the MM region. The shape of the potential energy curve did not change significantly (Figure S2 of the Supporting Information) because of the essentially same influence of the $[P_{D1}/P_{D2}]^{\bullet+}$ charge on Y_Z and D1-His190. Further detailed analysis, e.g., defining the $[P_{D1}/P_{D2}]^{\bullet+}$ molecule in the QM region, will be needed for further examination of this issue.

The idea that the ionic H-bond is important in the oxidation of Y_Z was put forward on a theoretical basis by Rappaport and Lavergne,[7] which was later supported by experimental studies.[6] So far as we know, this is the first clear demonstration of an exceptional H-bonding profile in the Y_Z-His190 dyad in PSII. Apparently, the PSII protein environment modulates (controls) the pK_a of the donor–acceptor pair of the system through the polar electrostatic environment. In the next section, to identify the structural origin of this pK_a modulation, we analyze the structural factors that affect the abnormal character of the H-bonding pattern.

A Cluster of Water Molecules near Y_Z and OEC That Contributed to the Short H-Bond. We calculated the $O_Y-N_{\varepsilon,His}$ distance to be 2.82 Å in a model system that consisted of Tyr and His side chains, in a vacuum (Table S4 of the Supporting Information), in agreement with the corresponding distances reported in previous model studies: 2.82,[16] 2.83,[17] and 2.88 Å.[18] These computational results demonstrated that the $O_{Y_Z}-N_{\varepsilon,His}$ distance in the 1.9 Å resolution structure is unusually short. In the model systems, we observed that the presence of a water molecule H-bonded to the OH group of Tyr resulted in a shorter $O_Y-N_{\varepsilon,His}$ distance of 2.73 Å (Table S4 of the Supporting Information).

In the PSII protein environment, two water molecules, W4 (O_Y-O_{W4} distance of 2.87 Å) and W7 (O_Y-O_{W7} distance of 2.62 Å), are H-bond distances from the hydroxyl O atom of Y_Z.[13] W4 is one of the two Ca-ligated water molecules of the OEC, and W7 is H-bonded to W6 and another Ca-ligated water W3. Both W3 and W6 are connected to W5. Thus, the four water molecules (W3 and W5–W7) form a diamond-shaped water cluster, where W7 is situated at the interface between the water cluster and Y_Z (Figure 2). Because a water H-bonded to the Tyr OH group played a role in shortening the $O_Y-N_{\varepsilon,His}$ distance in the model systems (Table S4 of the Supporting Information), we also investigated the influence of the water molecules on the $O_{Y_Z}-N_{\varepsilon,His}$ distance in the PSII protein environment.

Upon removal of all water molecules from PSII, the $O_{Y_Z}-N_{\varepsilon,His}$ distance significantly increased to 2.71 Å (Table 2). In particular, removal of five waters, W3–W7, near Y_Z (Figure 2) yielded a similar distance of 2.67 Å, which suggests that the water cluster plays a predominant role in specifying the short distance of 2.47 Å in the neutral [$Y_ZO\cdots\mathbf{H}\cdots N_\varepsilon$-His-$N_\delta\mathbf{H}\cdots O$=Asn] state. Nevertheless, it should be noted that the presence of only the water cluster cannot shorten the $O_{Y_Z}-N_{\varepsilon,His}$ distance. We calculated the $O_Y-N_{\varepsilon,His}$ distance to be 2.71 Å in a model system that consisted of Tyr and His side chains and the diamond-shaped cluster [W3 and W5–W7 (Figure 2)], in a vacuum (Figure S3 of the Supporting Information). Hence, not only the water cluster but also the PSII protein environment is needed to shorten the $O_{Y_Z}-N_{\varepsilon,His}$ distance. The PSII proteins not only provide a specific polar/charged environment but also are prerequisites for fixing the water cluster at the appropriate position and optimizing their dipoles.

Removal of W4 altered the $O_{Y_Z}-N_{\varepsilon,His}$ distance only marginally (2.51 Å). In contrast, removal of W7 considerably increased the $O_{Y_Z}-N_{\varepsilon,His}$ distance to 2.55 Å. Indeed, this change in the $O_{Y_Z}-N_{\varepsilon,His}$ distance was the largest upon removal of any single water investigated (Table 2). Thus, W7 plays a key role in shortening the $O_{Y_Z}-N_{\varepsilon,His}$ distance in the 1.9 Å structure

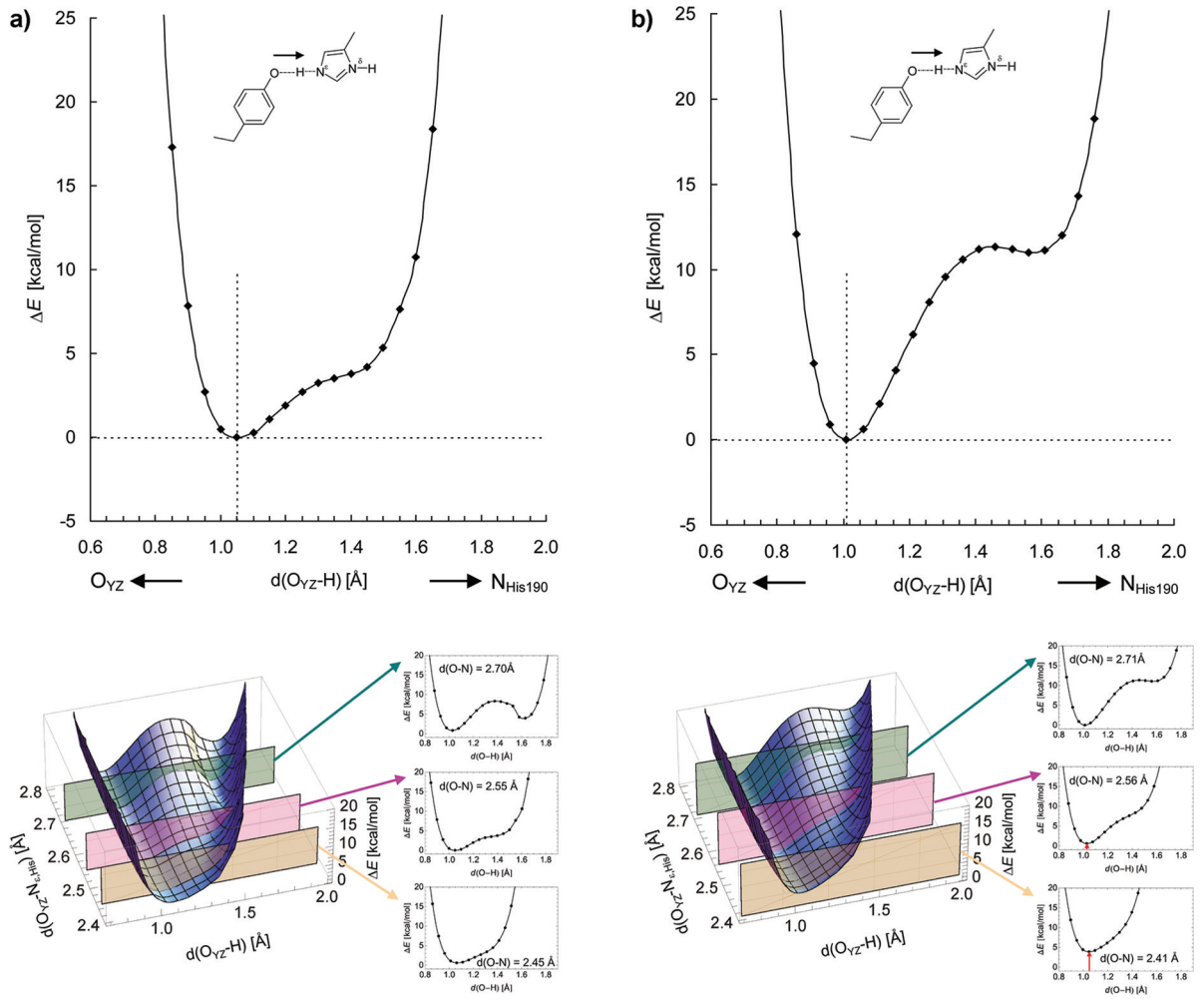

Figure 4. Influence of the deletion of water molecules on energy profiles along the PT coordinate for H-bond donor−acceptor pairs: deletion of (a) W7 and (b) all waters. ΔE describes the difference in energy relative to the energy minimum. Vertical dotted lines indicate the H atom position listed in Table 2. The red arrow indicates the energy difference from the energy minimum, although it is not always shown.

because of the stabilized H-bond orientation of W7 toward Y_Z, which is supported ultimately by the PSII protein dipoles via water molecules (Figure 5). One of the carboxyl O atoms of D1-Glu189 is fixed to Mn1, whereas the other carboxyl O atom is H-bond distance from W7; this leads to a strong fixation of an H atom of W7 on D1-Glu189. Indeed, mutations of D1-Glu189 altered the redox properties of Y_Z and the OEC, suggesting the involvement of D1-Glu189 in an H-bond network that modulates the properties of both Y_Z and the OEC.[29]

Remarkably, upon removal of W7, the highly anharmonic single-well potential curve (Figure 3a) obtained for the neutral [$Y_ZO\cdots\mathbf{H}\cdots N_{\varepsilon}$-His-$N_{\delta}\mathbf{H}\cdots O{=}$Asn] state ($O_{Y_Z}-N_{\varepsilon,His}$ distance of 2.47 Å) was altered dramatically to an asymmetric double-well potential curve (Figure 4a). The potential energy curve obtained in the absence of all water molecules resulted in the same type as an asymmetric double-well potential curve (Figure 4b). Undoubtedly, W7 is a key water that determines the short distance and the chemical properties (i.e., the type of potential energy curve) of the $O_{Y_Z}-N_{\varepsilon,His}$ bond. From a comparison between Figures 3a and 4a, it appears that the highly polarized W7 OH dipole elevates the energy specifically at the Y_Z moiety and promotes deprotonation of Y_Z, by stabilizing its deprotonated anionic state; this can be judged by the newly visible minima at the Y_Z moiety rather than the D1-His190 moiety upon removal of W7 (Figure 4a). Removing W7 leads to more stabilization of the Y_Z protonated form; this breaks the equal pK_a values of both Y_Z and D1-His190. Thus, the potential energy curve in the W7-depleted PSII (Figure 4a) is more asymmetric than that of native PSII (Figure 3a).

The activation energy of the Y_Z oxidation has been estimated to be ∼200 meV for OEC-depleted PSII.[6,30] Interestingly, a similar magnitude of the energy barrier appears upon removal of W7 (Figure 4a). It has been suggested that OEC-depleted PSII may have a different (not well-ordered) H-bond pattern near Y_Z versus that of intact PSII.[6−9] Because the side chain orientation of D1-Glu189, a ligand of the OEC (Figure 2), should be influenced by depletion of OEC, it may be reasonable to assume that OEC-depleted PSII may not possess W7 at the position of the intact PSII, possibly yielding an activation energy of ∼200 meV.

We also analyzed the potential energy profile by altering the $O_{Y_Z}-N_{\varepsilon,His}$ distance (Figure 4a, bottom). The potential energy curve with an $O_{Y_Z}-N_{\varepsilon,His}$ distance of ∼2.45 Å resembles that of a single-well potential but is not yet completely symmetric because of the slightly larger pK_a value of Y_Z with respect to that of D1-His190. More importantly, the energy minimum with an $O_{Y_Z}-N_{\varepsilon,His}$ distance of 2.45 Å is obviously energetically

dx.doi.org/10.1021/bi201366j | *Biochemistry* 2011, 50, 9836−9844

higher than that with an O_{Y_Z}–$N_{\varepsilon,His}$ distance of 2.55 Å. Thus, unless the pK_a values of the donor and acceptor moieties are similar, the bond becomes energetically unstable as the O_{Y_Z}–$N_{\varepsilon,His}$ distance decreases. Hence, in a comparison between Figures 3a and 4a, it appears that W7 plays a role in tuning the pK_a value of Y_Z in the native PSII so that the pK_a values of the donor and acceptor moieties are similar.

The orientations of other water molecules in the cluster are also strictly determined; e.g., W3 is supported by Ca, W5 by the backbone carbonyl of D1-Asp170, and W6 by the backbone carbonyl of D1-Phe182. As a result of this significantly polar environment, whose dipole orientations are specified by the PSII polar protein environment, the O_{Y_Z}–$N_{\varepsilon,His}$ distance is short, but only in the neutral [$Y_ZO\cdots\mathbf{H}\cdots N_\varepsilon$-His-$N_\delta$H] state. Thus, the H-bond pattern of water molecules near Y_Z is ultimately specified by the OEC and the ligands. Hence, OEC-depleted PSII, which is often used in experimental studies,[6,9] may have a different H-bond pattern near Y_Z than intact PSII (reviewed in ref 7). It has been suggested that Y_Z was not involved in a well-ordered H-bond in PSII core complexes depleted of the OEC,[8] or Y_Z was solvent accessible in OEC-depleted PSII.[9]

The orientation of the H-bonds described in Figure 5 was identical in both the $(O4)^{2-}(O5)H^-$ and $(O4)H^-(O5)H^-$

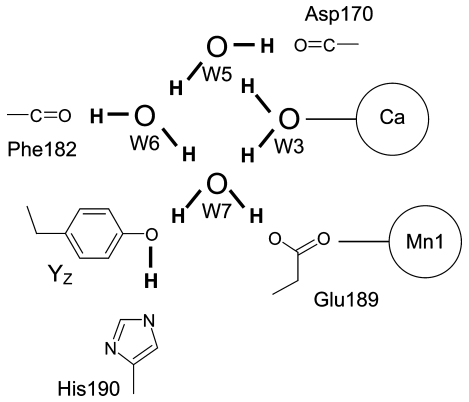

Figure 5. H-Bond network of the diamond-shaped water cluster near Y_Z. The orientations of the H atoms of water molecules are indicated by thick lines. W4 has been omitted for the sake of clarity. For numbering of water molecules, see ref 13.

models, irrespective of the protonation state of the OEC model. Hence, the well-organized electrostatic influence of the entire water cluster and PSII polar environment on Y_Z is the reason why removal of the single W7 molecule did not cause a more remarkable increase in the O_{Y_Z}–$N_{\varepsilon,His}$ distance. In turn, a much longer H-bond between Y_D (D2-Tyr160) and D2-His190 (2.74 Å[12]) in the 1.9 Å structure may be a result of its less polarized environment (e.g., the absence of the OEC and fewer water molecules and polar/charged amino acids near Y_D). On the other hand, for the energy profile of the bond, W7 is important for determining whether it is an asymmetric double-well potential curve or a highly anharmonic single-well potential curve. The specificity of W7 arises from its unusually high polarity, the position being fixed by the strongly ionized D1-Glu189, the ligand of the Mn1 atom of Mn_4CaO_5 (Figure 5). Therefore, the short distance between Y_Z and D1-His190 in the neutral [$Y_ZO\cdots\mathbf{H}\cdots N_\varepsilon$-His-$N_\delta$H] state is a fate of the O_2-evolving active PSII that possesses intact D1-Glu189 and Mn_4CaO_5.

CONCLUSIONS

The appropriate redox/protonation state of Y_Z and D1-His190 is a prerequisite for yielding the short O_{Y_Z}–$N_{\varepsilon,His}$ distance. The O_{Y_Z}–$N_{\varepsilon,His}$ distance of 2.47 Å was reproduced only in the neutral [$Y_ZO\cdots\mathbf{H}\cdots N_\varepsilon$-His-$N_\delta\mathbf{H}\cdots$O=Asn] state (Figure 1a). A different charge/protonation state, namely the positively charged $[Y_ZO\cdots\mathbf{H}\cdots N_\varepsilon$-His-$N_\delta\mathbf{H}\cdots$O=Asn$]^+$ state, yields a longer distance, 2.70 Å (Table 1). Thus, the short distance of 2.47 Å is not due to an artifact such as the absence of relaxation of the system. The geometry (O_{Y_Z}–$N_{\varepsilon,His}$ distance of 2.47 Å) can be obtained reversibly, using the $[Y_ZO\cdots\mathbf{H}\cdots N_\varepsilon$-His-$N_\delta\mathbf{H}\cdots$O=Asn$]^+$ geometry (O_{Y_Z}–$N_{\varepsilon,His}$ distance of 2.70 Å) but replacing the net charge with 0. These results suggest that the 1.9 Å structure is likely to be in the neutral [$Y_ZO\cdots\mathbf{H}\cdots N_\varepsilon$-His-$N_\delta\mathbf{H}\cdots$O=Asn] state.

In addition to the necessity of the appropriate charge/protonation state, the presence of the water cluster (Figures 2 and 5) is also a prerequisite for yielding the short H-bond between Y_Z and D1-His190. If there were no water molecules in PSII, the O_{Y_Z}–$N_{\varepsilon,His}$ distance should have been elongated to 2.71 Å (Table 2). W7 near Y_Z is strongly polarized by the OEC axial ligand Glu189 and appears to shorten the O_{Y_Z}–$N_{\varepsilon,His}$ distance the most among all of the water molecules. Nevertheless, removal of W7 resulted in an increase of the O_{Y_Z}–$N_{\varepsilon,His}$ distance to 2.55 Å, which is not sufficient to explain the elongated O_{Y_Z}–$N_{\varepsilon,His}$ distance of 2.71 Å in PSII depleted of all of the water molecules. Thus, the short O_{Y_Z}–$N_{\varepsilon,His}$ distance observed in the crystal structure is caused not only by W7 but also by dipoles induced by a combination of the water molecules associated with PSII, in particular those of the water cluster near Y_Z (W3–W7). The orientations of the H-bond dipoles of the water cluster ultimately originate from the PSII protein dipole orientations, e.g., D1-Glu189, Mn1, Ca, D1-Asp170, and D1-Phe182, suggesting that the polar environment of PSII is necessary to rationalize the short distance (Figure 5). On the other hand, because of the fixation of W7 by an OEC ligand, D1-Glu189, the polarity is strong enough to promote deprotonation of Y_Z. Thus, the short distance between Y_Z and D1-His190 in the neutral [$Y_ZO\cdots\mathbf{H}\cdots N_\varepsilon$-His-$N_\delta$H] state is a fate of the O_2-evolving active PSII that possesses intact D1-Glu189 and Mn_4CaO_5.

The presence of an ionic H bond between Y_Z and D1-His190 may be relevant to the experimental results that showed that Y_Z can be oxidized at liquid-helium temperatures in the S_0 and S_1 states (for a review, see ref 31). At liquid-helium temperatures, the proton motions would be blocked except those across ionic H-bonds. The observation of Y_Z oxidation at liquid-helium temperatures in the S_0 and S_1 states may suggest that at least the ionic H-bond between Y_Z and D1-His190 is maintained in these two states.

Biological functions of H bonds have attracted much attention in many protein systems during the past few decades. One of the typical examples is the so-called low-barrier H-bond (LBHB) hypothesis.[32,33] According to the initial idea proposed by Frey et al.[33] to explain the catalysis of serine proteases, the LBHB is generally defined as the state in which a hydrogen is equally shared between two heavy atoms inside a symmetric double-well potential and the zero-point energy of hydrogen is

close to the barrier height of PT. However, the relationship between the LBHB and its contribution to biological functions is not clear at present.[28,34−37] In particular, experimental evidence of the LBHB based only on the geometrical parameters (e.g., detailed X-ray coordinates) is inconclusive. Until now, even in a widely known system such as serine protease, recent ultra-high resolution crystal structures[37] as well as a series of ab initio QM/MM computations[35,38] do not support the LBHB hypothesis. In structural studies, the H bond in the His-Asp dyad of the serine protease is clearly demonstrated as a normal ionic H bond.[37] Also, QM/MM studies revealed that unusual physical properties of the His-Asp dyad are explained well on the basis of the concept of electrostatic interaction without invoking the LBHB.[35,38]

Considering the PT profile as well as the short atomic distance between Y_Z and D1-His190, again we can avoid the possibility of assuming the LBHB in PSII, and this unusual H-bond character can be explained well on the basis of the concept of an ionic H-bond.[28] Indeed, the idea that the ionic H-bond is important in the oxidation of Y_Z was suggested previously in refs 6 and 7. The major structural origin that enhances the short, ionic H bond is the presence and orientation of the water clusters around the OEC. Although the PSII protein environment favors a rather symmetric PT profile (which implies the matched pK_a between the donor and acceptor[36]), how the D1/D2 heterodimer or other redox-active cofactors modulate (or controls) the pK_a of these key residues remains elusive at present. The state in which both residues have equal pK_a values and the proton is delocalized between the two residues may have an advantage in effectively controlling the electron transfer process. In future studies, we will address this fundamental question as well as the missing link between structural parameters and the molecular properties that facilitate electron transfer.

■ ASSOCIATED CONTENT

Supporting Information

Atomic charges, optimized geometries, and computational results of the model systems. This material is available free of charge via the Internet at http://pubs.acs.org.

■ AUTHOR INFORMATION

Corresponding Author

*Address: 202 Building E, Career-Path Promotion Unit for Young Life Scientists, Graduate School of Medicine, Kyoto University, Yoshida-Konoe-cho, Sakyo-ku, Kyoto 606-8501, Japan. Telephone: +81-75-753-9286. Fax: +81-75-753-9281. E-mail: hiro@cp.kyoto-u.ac.jp.

Funding

This research was supported by the JST PRESTO program (H.I.), a Grant-in-Aid for Science Research from the Ministry of Education, Science, Sport and Culture of Japan (21770163 to H.I. and 22740276 to K.S.), the Special Coordination Fund for Promoting Science and Technology of MEXT (H.I.), the Takeda Science Foundation (H.I.), and a Kyoto University Step-up Grant-in-Aid for young scientists (H.I.).

■ ABBREVIATIONS

Chl*a*, chlorophyll *a*; LBHB, low-barrier hydrogen bond; OEC, oxygen-evolving complex; PSII, Photosystem II; QM/MM, quantum mechanical/molecular mechanical; Y_D, redox-active tyrosine D2-Tyr160; Y_Z, redox-active tyrosine D1-Tyr161.

■ REFERENCES

(1) Prokhorenko, V. I., and Holzwarth, A. R. (2000) Primary process and structure of the photosystem II reaction center: A photon echo study. *J. Phys. Chem. B 104*, 11563−11578.

(2) Ishikita, H., Biesiadka, J., Loll, B., Saenger, W., and Knapp, E. W. (2006) Cationic state of accessory chlorophyll and electron transfer through pheophytin to plastoquinone in photosystem II. *Angew. Chem., Int. Ed. 45*, 1964−1965.

(3) Renger, G., and Renger, T. (2008) Photosystem II: The machinery of photosynthetic water splitting. *Photosynth. Res. 98*, 53−80.

(4) Noguchi, T., Inoue, Y., and Tang, X.-S. (1997) Structural coupling between the oxygen-evolving Mn cluster and a tyrosine residue in photosystem II as revealed by Fourier transform infrared spectroscopy. *Biochemistry 36*, 14705−14711.

(5) Berthomieu, C., Hienerwadel, R., Boussac, A., Breton, J., and Diner, B. A. (1998) Hydrogen bonding of redox-active tyrosine Z of photosystem II probed by FTIR difference spectroscopy. *Biochemistry 37*, 10547−10554.

(6) Rappaport, F., Boussac, A., Force, D. A., Peloquin, J., Brynda, M., Sugiura, M., Un, S., Britt, R. D., and Diner, B. A. (2009) Probing the coupling between proton and electron transfer in photosystem II core complexes containing a 3-fluorotyrosine. *J. Am. Chem. Soc. 131*, 4425−4433.

(7) Rappaport, F., and Lavergne, J. (2001) Coupling of electron and proton transfer in the photosynthetic water oxidase. *Biochim. Biophys. Acta 1503*, 246−259.

(8) Tommos, C., Tang, X.-S., Warncke, K., Hoganson, C. W., Styring, S., McCracken, J., Diner, B. A., and Babcock, G. T. (1995) Spin-density distribution, conformation, and hydrogen bonding of the redox-active tyrosine Y_Z in photosystem II from multiple-electron magnetic-resonance spectroscopies: Implications for photosynthetic oxygen evolution. *J. Am. Chem. Soc. 117*, 10325−10335.

(9) Hays, A.-M. A., Vassiliev, I. R., Golbeck, J. H., and Debus, R. J. (1999) Role of D1-His190 in the proton-coupled oxidation of tyrosine Y_Z in manganese-depleted photosystem II. *Biochemistry 38*, 11851−11865.

(10) Rutherford, A. W., and Boussac, A. (2004) Water photolysis in biology. *Science 303*, 1782−1784.

(11) Haumann, M., Liebisch, P., Muller, C., Barra, M., Grabolle, M., and Dau, H. (2005) Photosynthetic O_2 formation tracked by time-resolved X-ray experiments. *Science 310*, 1019−1021.

(12) Umena, Y., Kawakami, K., Shen, J.-R., and Kamiya, N. (2011) Crystal structure of oxygen-evolving photosystem II at 1.9 Å resolution. *Nature 473*, 55−60.

(13) Kawakami, K., Umena, Y., Kamiya, N., and Shen, J.-R. (2011) Structure of the catalytic, inorganic core of oxygen-evolving photosystem II at 1.9 Å resolution. *J. Photochem. Photobiol., B 104*, 9−18.

(14) Loll, B., Kern, J., Saenger, W., Zouni, A., and Biesiadka, J. (2005) Towards complete cofactor arrangement in the 3.0 Å resolution structure of photosystem II. *Nature 438*, 1040−1044.

(15) Guskov, A., Kern, J., Gabdulkhakov, A., Broser, M., Zouni, A., and Saenger, W. (2009) Cyanobacterial photosystem II at 2.9-Å resolution and the role of quinones, lipids, channels and chloride. *Nat. Struct. Mol. Biol. 16*, 334−342.

(16) Faller, P., Goussias, C., Rutherford, A. W., and Un, S. (2003) Resolving intermediates in biological proton-coupled electron transfer: A tyrosyl radical pair to proton movement. *Proc. Natl. Acad. Sci. U.S.A. 100*, 8732−8735.

(17) Yan, S., Kang, S., Hayashi, T., Mukamel, S., and Lee, J. Y. (2009) Computational studies on electron and proton transfer in phenol-imidazole-base triads. *J. Comput. Chem. 31*, 393−402.

(18) Un, S., Boussac, A., and Sugiura, M. (2007) Characterization of the tyrosine-Z radical and its environment in the spin-coupled S_2Tyr_Z* state of photosystem II from *Thermosynechococcus elongatus*. *Biochemistry 46*, 3138−3150.

(19) Saito, K., Ishida, T., Sugiura, M., Kawakami, K., Umena, Y., Kamiya, N., Shen, J.-R., and Ishikita, H. (2011) Distribution of the

cationic state over the chlorophyll pair of photosystem II reaction center. *J. Am. Chem. Soc. 133*, 14379−14388.
(20) Brooks, B. R., Bruccoleri, R. E., Olafson, B. D., States, D. J., Swaminathan, S., and Karplus, M. (1983) CHARMM: A program for macromolecular energy minimization and dynamics calculations. *J. Comput. Chem. 4*, 187−217.
(21) MacKerell, A. D. Jr., Bashford, D., Bellott, R. L., Dunbrack, R. L. Jr., Evanseck, J. D., Field, M. J., Fischer, S., Gao, J., Guo, H., Ha, S., Joseph-McCarthy, D., Kuchnir, L., Kuczera, K., Lau, F. T. K., Mattos, C., Michnick, S., Ngo, T., Nguyen, D. T., Prodhom, B., Reiher, W. E. III, Roux, B., Schlenkrich, M., Smith, J. C., Stote, R., Straub, J., Watanabe, M., Wiorkiewicz-Kuczera, J., Yin, D., and Karplus, M. (1998) All-atom empirical potential for molecular modeling and dynamics studies of proteins. *J. Phys. Chem. B 102*, 3586−3616.
(22) Bayly, C. I., Cieplak, P., Cornell, W. D., and Kollman, P. A. (1993) A well-behaved electrostatic potential based method using charge restraints for deriving atomic charges: The RESP model. *J. Phys. Chem. 97*, 10269−10280.
(23) *Jaguar*, version 7.5 (2008) Schrödinger, LLC, New York.
(24) Luber, S., Rivalta, I., Umena, Y., Kawakami, K., Shen, J.-R., Kamiya, N., Brudvig, G. W., and Batista, V. S. (2011) S_1-state model of the O_2-evolving complex of photosystem II. *Biochemistry 50*, 6308−6311.
(25) *QSite*, version 5.6 (2010) Schrödinger, LLC, New York.
(26) Haumann, M., and Junge, W. (1999) Photosynthetic water oxidation: A simplex-scheme of its partial reactions. *Biochim. Biophys. Acta 1411*, 86−91.
(27) Haumann, M., Mulkidjanian, A., and Junge, W. (1999) Tyrosine-Z in oxygen-evolving photosystem II: A hydrogen-bonded tyrosinate. *Biochemistry 38*, 1258−1267.
(28) Perrin, C. L., and Nielson, J. B. (1997) "Strong" hydrogen bonds in chemistry and biology. *Annu. Rev. Phys. Chem. 48*, 511−544.
(29) Debus, R. J., Campbell, K. A., Pham, D. P., Hays, A. M., and Britt, R. D. (2000) Glutamate 189 of the D1 polypeptide modulates the magnetic and redox properties of the manganese cluster and tyrosine Y_Z in photosystem II. *Biochemistry 39*, 6275−6287.
(30) Ahlbrink, R., Haumann, M., Cherepanov, D., Bogershausen, O., Mulkidjanian, A., and Junge, W. (1998) Function of tyrosine Z in water oxidation by photosystem II: Electrostatical promotor instead of hydrogen abstractor. *Biochemistry 37*, 1131−1142.
(31) Petrouleas, V., Koulougliotis, D., and Ioannidis, N. (2005) Trapping of metalloradical intermediates of the S-states at liquid helium temperatures. Overview of the phenomenology and mechanistic implications. *Biochemistry 44*, 6723−6728.
(32) Cleland, W. W., and Kreevoy, M. M. (1994) Low-barrier hydrogen bonds and enzymic catalysis. *Science 264*, 1887−1890.
(33) Frey, P. A., Whitt, S. A., and Tobin, J. B. (1994) A low-barrier hydrogen bond in the catalytic triad of serine proteases. *Science 264*, 1927−30.
(34) Warshel, A., Papazyan, A., and Kollman, P. A. (1995) On low-barrier hydrogen bonds and enzyme catalysis. *Science 269*, 102−106.
(35) Ishida, T., and Kato, S. (2003) Theoretical perspectives on the reaction mechanism of serine proteases: The reaction free energy profiles of the acylation process. *J. Am. Chem. Soc. 125*, 12035−12048.
(36) Schutz, C. N., and Warshel, A. (2004) The low barrier hydrogen bond (LBHB) proposal revisited: The case of the Asp...His pair in serine proteases. *Proteins 55*, 711−723.
(37) Fuhrmann, C. N., Daugherty, M. D., and Agard, D. A. (2006) Subangstrom crystallography reveals that short ionic hydrogen bonds, and not a His-Asp low-barrier hydrogen bond, stabilize the transition state in serine protease catalysis. *J. Am. Chem. Soc. 128*, 9086−9102.
(38) Ishida, T. (2006) Low-barrier hydrogen bond hypothesis in the catalytic triad residue of serine proteases: Correlation between structural rearrangement and chemical shifts in the acylation process. *Biochemistry 45*, 5413−5420.